COSPAR COLLOQUIA SERIES Volume 11

THE OUTER HELIOSPHERE: THE NEXT FRONTIERS

Edited by
K. SCHERER, H. FICHTNER,
H.-J. FAHR AND E. MARSCH

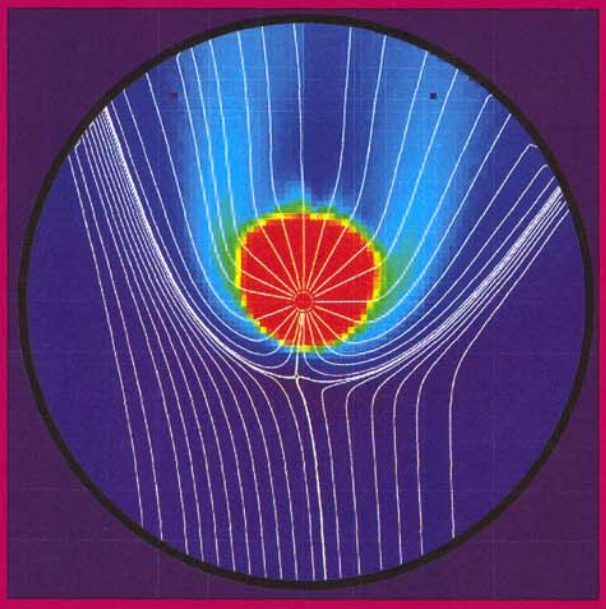

Pergamon

THE OUTER HELIOSPHERE:

THE NEXT FRONTIERS

Proceedings of COSPAR Colloquium
held in Potsdam, Germany
24-28 July 2000

Edited by

Klaus Scherer
dat-hex, Katlenburg-Lindau, Germany

Horst Fichtner
Institut für Theoretische Physik IV, Ruhr-Universität Bochum, Bochum, Germany

Hans Jörg Fahr
Institut Für Astrophysik und extraterrstrische Forschung, Universität Bonn, Bonn, Germany

Eckart Marsch
Max-Planck-Institut für Aeronomie, Katlenburg-Lindau, Germany

2001

PERGAMON
An Imprint of Elsevier Science

Amsterdam – London – New York – Oxford – Paris – Shannon – Tokyo

Mapping the Heliopause in EUV

Mike Gruntman

Department of Aerospace and Mechanical Engineering, MC-1191
University of Southern California, Los Angeles, CA 90089-1191

We know very little about the heliopause, a boundary that separates the solar wind and the galactic plasma of the local interstellar medium (LISM), with the direct experimental data next to nonexistent. We propose to explore the heliopause remotely, from 1 AU by an observer outside of the geocorona. Interstellar plasma ions beyond the heliopause would glow under solar extreme-ultraviolet (EUV) radiation in the resonance lines of oxygen (83.4 nm) and helium (30.4 nm). The measurements of this glow would map the heliopause. Heliopause mapping in EUV is a way to remotely explore the heliospheric interface region and the LISM ionization state and to probe the asymmetry of the interstellar magnetic field.

1. HELIOPAUSE

The interaction of our star, the Sun, with the surrounding local interstellar medium (LISM) leads to the buildup of the heliosphere, the region where the Sun controls the state and behavior of the plasma environment. The heliosphere is a complicated phenomenon where solar wind and interstellar plasmas, neutral interstellar gas, magnetic fields, anomalous and galactic cosmic rays, and energetic neutral atoms play prominent roles (Figure 1).

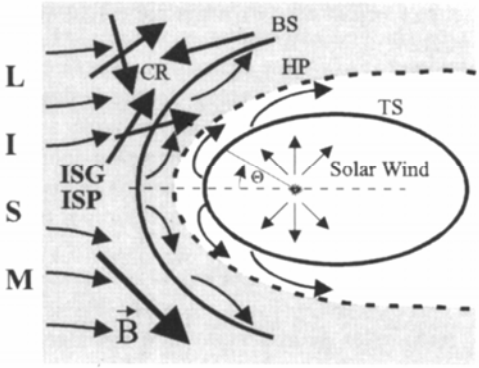

Figure 1. Possible solar wind interaction (two-shock model) with the LISM: TS - termination shock; HP-heliopause; BS - bow shock; CR - cosmic rays; ISP(G) -interstellar plasma (gas); B - magnetic field. Interstellar plasma flows outside the heliopause (gray area). Angle θ is counted from the upwind direction.

Experimental data on the sun-LISM interaction region are exceptionally scarce, mostly indirect and often ambiguous. We know very little about the heliopause, a boundary that separates the solar wind plasma and the interstellar plasma.[1]

Many important questions remain unanswered, for example: What is the distance to and shape of the heliopause? What is the ionization state of interstellar gas in the LISM? What is the direction and magnitude of the interstellar magnetic field? Is the interstellar wind subsonic or supersonic? Is a bow shock formed in front of the heliosphere?

Voyager 1, now approaching 80 AU, is expected to cross the termination shock and explore the heliospheric sheath properties in one point-direction. The spacecraft may not however reach the heliopause by the end of the mission in ~2025.

The interstellar wind, solar wind latitudinal variations, and interstellar magnetic field make the heliosphere asymmetric. Only remote techniques, complemented by the "ground truth" Voyager and future Interstellar Probe in-situ measurements, can provide a global view of the time-varying three-dimensional heliosphere on a continuous basis.

The heliopause separates the interstellar and solar wind plasmas with the number densities 2 orders of magnitude different. Figure 2 illustrates the dependence of the plasma number density[2] on the heliocentric distance in the approximately upwind direction (with respect to the interstellar wind). The plasma density rapidly decreases with the expansion of the solar wind. Interstellar plasma cannot cross the heliopause and flows around it. One can imagine the sun surrounded by an interstellar ion "wall" beyond the empty cavity, the "heliopause moat," limited by the heliopause boundary. Is the heliopause stable under such conditions?

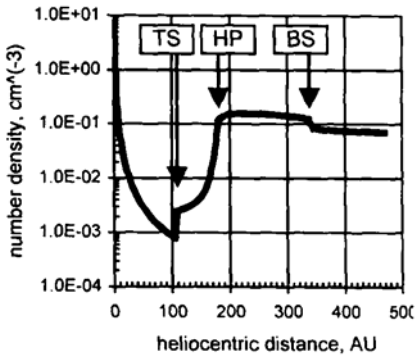

Figure 2. Typical plasma number density in the upwind direction. The arrows indicate the positions of the termination shock (TS), heliopause (HP), and bow shock (BS).

This heliopause moat suggests a way of remote, from 1 AU, mapping of the heliopause.[3,4] Singly charged interstellar ions (He^+, O^+) would scatter the corresponding solar extreme-ultraviolet (EUV) line emissions. Measurements of this scattered radiation, the LISM plasma glow, would open an access to the heliopause and the region beyond. Heliopause imaging would map the heliopause and provide an important insight into the LISM ionization state and the asymmetry of the interstellar magnetic field. Heliopause EUV mapping, combined with the heliosheath plasma imaging in energetic neutral atoms,[5,6,7,8] will explore in detail the three-dimensional time-varying region of the sun-LISM interaction.

2. HELIOPAUSE MAPPING

Interstellar neutral atoms are unsuitable for heliopause mapping because they penetrate deep into the heliosphere. Most of the glow of heliospheric neutrals, as seen by an observer near 1 AU, would originate within the 10-AU region. Interstellar protons cannot be imaged optically at all. Interstellar helium (He^+) and oxygen (O^+) ions are ideally suited for heliopause mapping. Helium is the most abundant interstellar gas constituent (~10%) after hydrogen, with the exceptionally bright corresponding solar line (30.4 nm). Measurement of the ionization state of interstellar helium will provide an important insight into heating and cooling of the LISM. Oxygen is the most abundant interstellar gas minor constituent (~0.1%). The ionization states of hydrogen and oxygen are tightly coupled by efficient charge exchange. Therefore, the experimental determination of the ionization state of oxygen will establish the ionization state of hydrogen.

For an observer at 1 AU looking in the antisolar direction, the radiance (photon cm^{-2} s^{-1} sr^{-1}) $F(\theta)$ is an integral along the line of sight

$$F(\theta) = \frac{1}{4\pi} \int_{R_E}^{\infty} N_{I+}(R,\theta)\, g_I(R)\, dR$$

where the g-factor (scattering rate per ion per second) $g_I(R)$ depends on the distance from the sun, $N_{I+}(R,\theta)$ is the local ion number density, R_E = 1 AU, and the scattering phase function is assumed isotropic.

For a simplified case of 1) vanishing ion number density inside the heliopause ($R < R_{HP}$) and 2) interstellar plasma (beyond the heliopause) at rest with a uniform number density and constant temperature, the radiance would be

$$F(\theta) = \frac{N_{I+}\, g_{I,E}\, R_E^2}{4\pi} \quad \frac{1}{R_{HP}}$$

where $g_{I,E}$ is the g-factor at 1 AU. The sky brightness is thus inversely proportional to the distance to the heliopause in the direction of observation. Measuring the directional dependence (imaging) of the interstellar plasma glow is a way to establish the size and shape of the heliopause. The detailed temperature, velocity and number density flow fields of the LISM plasma are needed for accurate treatment of the problem, and the g-factors should be calculted for the specific local velocity distribution functions of the ions.

The plasma flow field was calculated for this work by Vladimir Baranov and co-workers in the Russian Academy of Sciences, Moscow using their two-shock sun-LISM interaction model[2] with the following LISM parameters (at infinity): velocity, 25 km s^{-1}; temperature, 5672 K; electron (proton) number density, n_e = 0.07 cm^{-3}; neutral hydrogen number density, n_H = 0.14 cm^{-3}. The solar wind was assumed to flow spherically symmetric with a velocity of 450 km s^{-1} and a number density of 7 cm^{-3} at 1 AU. Interstellar helium and oxygen abundances were assumed 0.1 and 7×10^{-4}, respectively, by the number of atoms relative to hydrogen.

3. SOLAR LINES, BACKGROUND, AND FOREGROUND

The solar emissions in the He^+ and O^+ resonance lines are well known.[9,10] Figure 3 shows the line profiles used in this work. The total solar flux in the helium line (30.4 nm) was assumed to be 6.0×10^9 cm^{-2} s^{-1} at 1 AU and the line FWHM 0.01 nm (0.1 Å).[9] An oxygen ion O^+ has a triplet transition at 83.2754, 83.3326, and 83.4462 nm. Both the solar emission O^+ and the nearby O^{2+} multiplet could excite moving interstellar and heliospheric O^+ ions. The total solar flux[10] in all the lines was assumed to be 5.3×10^8 cm^{-2} s^{-1}. The continuum contribution is 1.8×10^8 cm^{-2} s^{-1} nm^{-1} and 4.0×10^8 cm^{-2} s^{-1} nm^{-1} for the helium and oxygen lines, respectively. This contribution is important for the glow of oxygen ions, but unimportant for helium.

There are two other major sources of radiation at 30.4 and 83.4 nm, the solar wind produced foreground and the galactic background. The feasibility of heliopause mapping critically depends on spectral properties and relative strength (brightness) of this interfering radiation. One requires the LISM plasma glow (the "heliopause glow") to be brighter and/or spectrally separated from the background and foreground radiation.

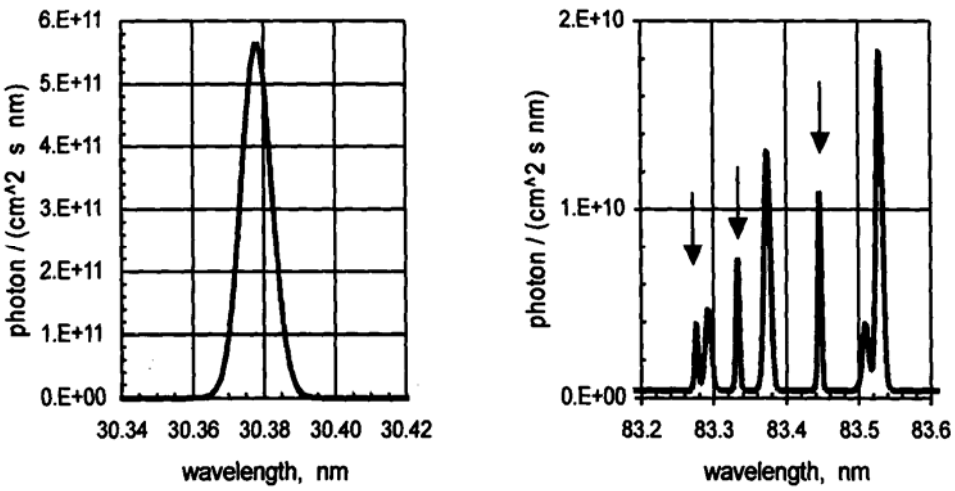

Figure 3. Solar emissions in the He^+ (30.4 nm) and O^+ (83.4 nm) resonance lines used in this work. Arrows mark the OII triplet lines; other nearby lines are of the OIII multiplet. The continuum is important for the oxygen irradiance, but unimportant for helium.

The glow of the He^+ and O^+ ions in the solar wind would produce the foreground radiation. These ions are produced by ionization of interstellar neutrals penetrating the heliosphere. The newly formed ions are picked up by the solar wind flow and carried to the termination shock as the pickup ions.[11,12] The pickup ions are singly charged and characterized by a spherical shell velocity distribution function. The glow of the pickup ions is the line radiation spectrally similar to the LISM plasma glow.

We calculated the number densities of the pickup ions describing the inflowing interstellar neutral helium and oxygen by the hot model. Interstellar helium is only slightly affected by the crossing of the heliospheric intreface region. In contrast, the properties of interstellar oxygen are significantly modified by the crossing, which requires use of modified gas parameters at infinity. The details of the calculations can be found elsewhere.[4,13] The glow of the pickup ions was calculated similarly to that of the LISM plasma beyond the heliopause. We used the spherical shell velocity distribution function in calculations of the g-factors. The observed asymmetry[14,15] of the ion distribution function would only slightly modify the expected pickup ion glow and was disregarded in this work.

At 30.4 nm, there is another important source of the foreground, viz. the emissions produced in charge exchange between the solar wind alpha-particles (He^{2+}) and heliospheric atomic hydrogen. The existence of this emission was known for some time,[16,17] but only recently it was analyzed in detail.[18] This emission is spectrally separated from the glow of the LISM and pickup ions and would not interfere with heliopause mapping (see below). We also note here that the all-sky images in the charge-exchange emissions will remotely reveal the three-dimensional solar wind flow properties everywhere in the heliosphere, including in the regions over the sun's poles and on the other (from the observer) side of the sun.[18]

Two main sources of the EUV background are the radiation emitted by hot interstellar plasmas (diffuse galactic background) and by the stars (stellar radiation field). The stellar

radiation field is a continuum with negligible line emissions, while hot plasmas emit a continuum with prominent line emissions. The stellar radiation dominates the EUV continuum background at wavelengths > 20 nm.[19,20] The total (at least 90% complete) continuum radiation field is ~13 photon cm^{-2} s^{-1} nm^{-1} and ~9.3 photon cm^{-2} s^{-1} nm^{-1} at 30.4 nm and 83.4 nm, respectively.[20]

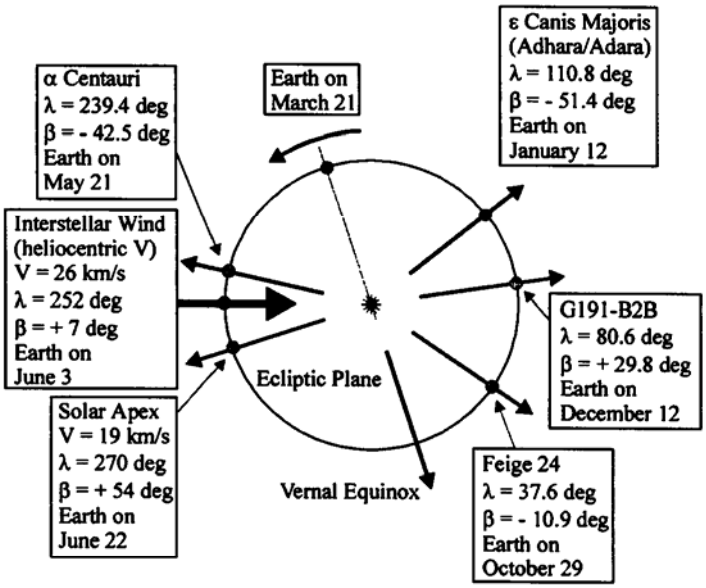

Figure 4. Projections on the ecliptic plane of the most important stellar sources (Adhara, G191-B2B, and Feige 24) of the background radiation at 30.4 nm and 83.4 nm; λ and β are the ecliptic longitude and latitude, respectively. Also shown are the interstellar wind, solar apex, and the closest star, α Centauri.

The stellar EUV background radiation is highly anisotropic.[20] A single bright star, ε Canis Majoris (Adhara or Adara), produces most of the radiation at 83.4 nm. Two white dwarfs, Feige 24 and G191-B2B dominate the background at 30.4 nm.[20] For isotropic background, the estimated stellar radiation[20] field translates into the ~1.3×10^{-2} mR/nm and ~9.3×10^{-3} mR/nm at 30.4 nm and 83.4 nm, respectively. (1 Rayleigh = 1 R = 10^3 mR = 10^6 μR = $10^6/(4\pi)$ phot cm^{-2} s^{-1} sr^{-1}.) For observations in the directions other than toward these bright sources (Figure 4), the stellar continuum background would be significantly smaller.

Hot (~10^6 K) interstellar plamas efficiently emit EUV radiation that includes both the line emissions and continuum. The sun is embedded in a relatively small, a few parsec long, and dense (~0.1 cm^{-3}) local interstellar cloud. This local interstellar cloud (LIC), our LISM, is too cold (~7000 K) to emit EUV radiation. LIC is positioned in the center of a region, the Local Bubble, filled with hot and dilute plasmas. These plasmas would emit the EUV radiation that after partial absorption in the LIC would reach the sun.

The hot plasma EUV background (line emissions and continuum) was calculated using a standard plasma emission model[21] with the temperaure 10^6 K, emission measure 0.0006 cm^{-6} pc, and 10^{18} cm^{-2} column density of the absorbing LIC hydrogen.[18]

Charge exchange of the solar wind alpha-particles would form, with some probability, single charged helium ions in the metastable state.[18] The metastable ions would decay by a two-photon emission process contributing to the background for λ>30.4 nm. Actually, this two-photon decay would dominate the continuum background in most directions in the 35-90

nm wavelength range.[18] The contributions from various sources to the background EUV continuum are summarized in Table 1.

Table 1
Background EUV continuum spectral radiance, mR/nm

Wavelength	Stellar field (isotropic)	Local Buble plasma emission	Solar Wind charge exchange emission
30.4 nm	1.3×10^{-2}	6.7×10^{-4}	0
83.4 nm	9.3×10^{-3}	4.3×10^{-6}	$(1.0\text{-}2.8) \times 10^{-3}$

4. RADIANCE AT 30.4 NM AND 83.4 NM

Figure 5 shows the calculated radiance of the glow of the LISM plasma beyond the heliopause and the glow of the pickup ions. The helium glow is much brighter (milli-Rayleighs) as compared to the oxygen glow (micro-Rayleighs). The initial slight increase of the LISM plasma brightness with the angle θ is due to the Doppler effect as the velocity radial component diminishes in the plasma turning around the heliopause.The glow falls as the heliopause moves away from the sun and the Doppler effect reduces the g-factor.

If the plasma had the constant number density, velocity and temperature beyond the heliopause, then the glow angular dependence would have been inversely proportional to the distance to the heliopause. This latter inverse radial dependence is shown by the solid curves. The difference between the solid curves and the calculated radiance (empty circles) illustrates the sensitivity of heliopause mapping to the plasma flow field beyond the heliopause.

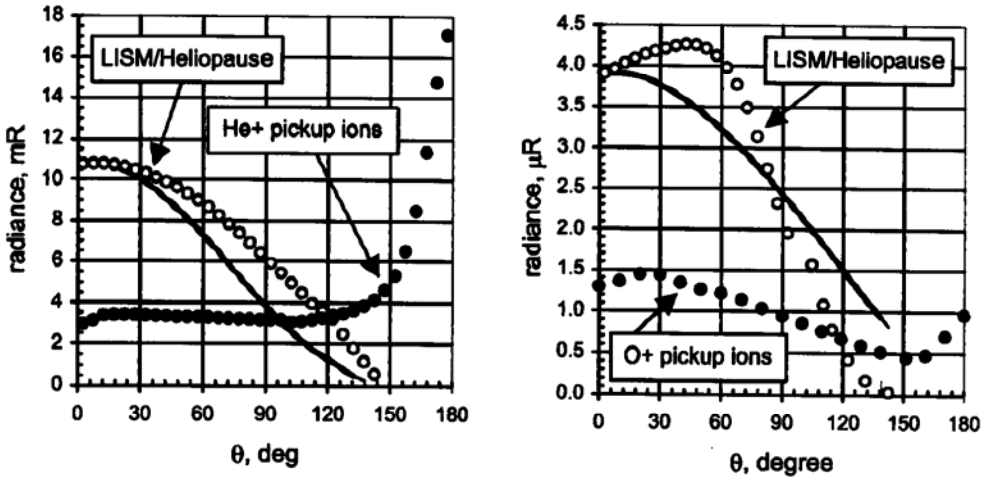

Figure 5. Glow at 30.4 nm and 83.4 nm of the LISM plasma beyond the heliopause and the solar wind pickup ions. The solid curves are the function $1/R_{HP}$ normalized at $\theta = 0$, R_{HP} is the distance to the heliopause.

The assumed ion-to-neutral ratios were 0.3125 and 0.5 for helium and oxygen, respectively. The brightness of the LISM plasma glow is roughly proportional to the number density of the interstellar gas ionized component, while the pickup ion glow is roughly proportional to the number density of the neutral component. Figure 6 illustrates this effect for oxygen,[4] showing the angular dependence of the radiance for three different ion-to-neutral ratios, 1:2, 1:1, and 2:1. Helium glow properties exhibit a similar dependence on the ionization state. By measuring the upwind-to-downwind brightness ratio one would establish the ionization state of helium and oxygen.

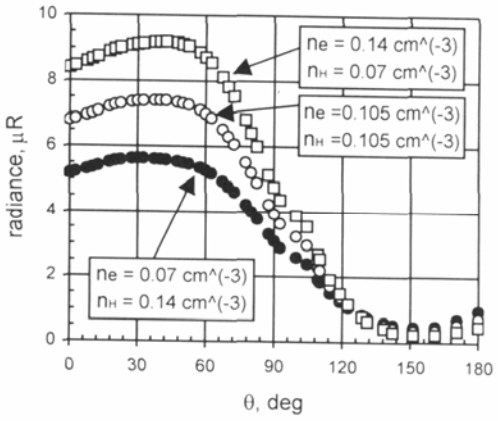

Figure 6. Sky radiance directional dependence at 83.4 nm for various ionization states of the LISM. Interstellar oxygen is assumed ionized similarly to hydrogen. Total LISM number density is 0.21 cm^{-3}, and the oxygen relative abundance is 7×10^{-4}.

5. SPECTRAL RADIANCE

The expected spectral radiance at 30.4 nm is shown in Figure 7. The LISM plasma and pickup ion glows are in practically the same spectral range. Most of the adjacent plasma line emissions (from the Local Bubble) are produced by interstellar OIII, AlIX, and SiXI ions. The continua of the plasma emission and the stellar radiation field are negligible. The

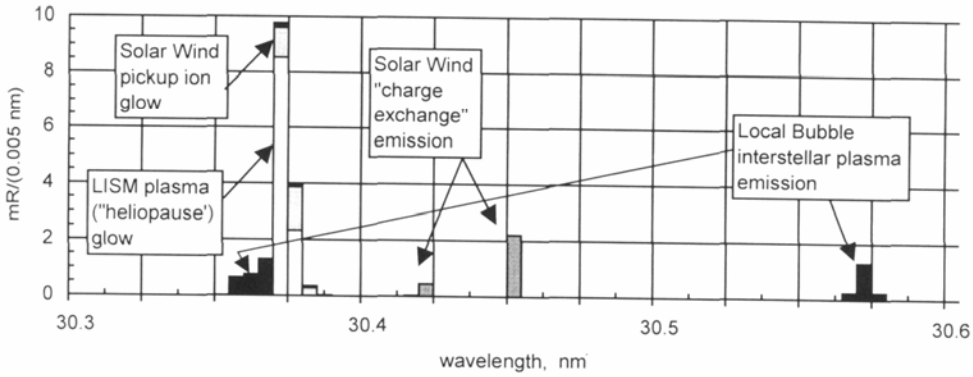

Figure 7. Typical spectral radiance at 30.4 nm. The glow of the LISM plasma beyond the heliopause is shown as white (empty) bars. Also shown are the pickup ion glow (light gray bars), Local Bubble interstellar emissions (black bars), and the solar wind charge-exchange emission (dark gray bars; the two peaks correspond to the fast/polar and slow/ecliptic solar wind).

Doppler shifted solar wind charge-exchange emissions[18] are clearly spectrally separated from other emissions. Measurements of the heliopause glow with the spectral resolution ~0.025 nm would allow one to eliminate the interfering contributions of the solar wind emissions. In order to efficiently remove the contributions of the interstellar lines, one would require the resolution of 0.005 nm.

Figure 8 shows the spectral radiance at 83.4 nm. The glows of the LISM plasma and the solar wind pickup ions are of comparable total radiance of several milli-Rayleighs. However, the spectral radiance of the LISM plasma glow is about one order of magnitude brighter since it is concentrated in the narrower spectral range (Figure 8a,b). The continuum radiation due to two-photon decay of the metastable ions in the solar wind[18] and stellar radiation field[20] are not negligible (Table 1). The combined spectral radiance from all sources is shown in Figure 8c for a typical continuum 0.16 μR/(0.01nm).

The glow measurements with a 0.01-nm spectral resolution would allow identification of the contributions from the LISM plasma and from the pickup ions. Much modest resolution of ~0.1 nm, should provide the combined glow radiance.

The recently developed EUV spectrometers EURD advanced the sensitivity of the diffuse radiation detection to 1 mR.[22] The new space mission CHIPS, presently under preparation, will study the diffuse galactic radiation with a sensitivity of ~1 mR/line at $\lambda < 26$ nm. The proposed heliopause mapping requires, however, significantly higher (a factor of 100) spectral resolution at 30.4 nm and significantly higher sensitivity (a factor of 100) at 83.4 nm. Development of diffuse EUV radiation spectrometers with such advanced performance characteristics is a challenging but not impossible task.

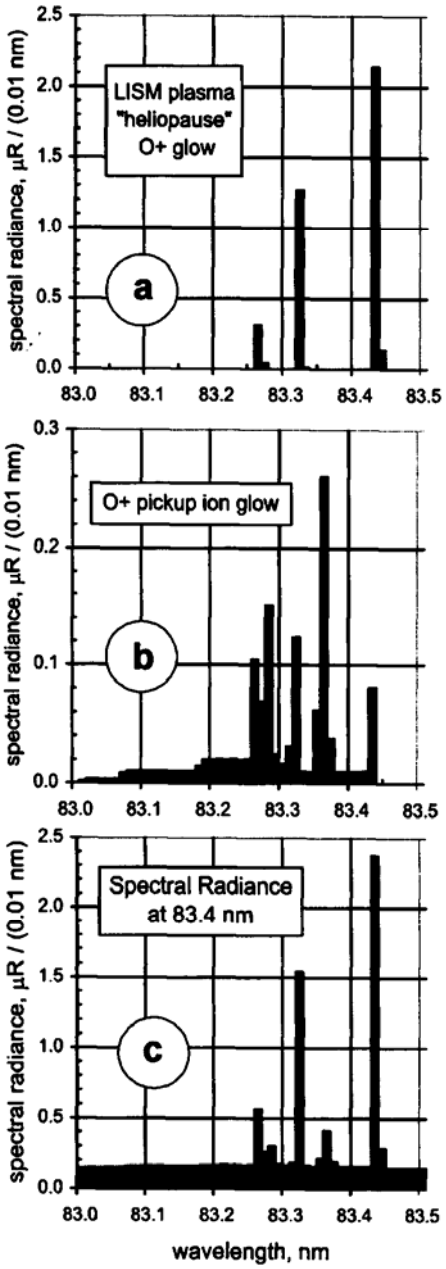

Figure 8. Spectral radiance at 83.4 nm. a) LISM plasma glow; b) pickup ions glow; c) combined spectral radiance including the continuum.

Mapping the all-sky radiance at 30.4 nm and 83.4 nm will establish the distance to and shape of the heliopause. The ionization states of interstellar helium and oxygen (and correspondingly hydrogen) will be obtained from such measurements. The asymmetry of the insterstellar magnetic field would also be pronounced and identified in the all-sky maps. The geocorona is bright at 30.4 nm and 83.4 nm, and too many photons would reach the night side through multiple scattering.[23] The heliopause mapping experiment can be performed only from a spacecraft outside the geocorona.

REFERENCES:

1. S.T. Suess, Rev. Geophys., 28, 97-115, 1990.
2. V.B. Baranov and Yu. G. Malama, J. Geophys. Res., 98, 15157-15163, 1993.
3. M. Gruntman and H.J. Fahr, 25, 1261-1264, 1998.
4. M. Gruntman and H.J. Fahr, J. Geophys. Res., 105, 5189-5200, 2000.
5. M.A. Gruntman, Planet. Space Sci., 40, 439-445, 1992.
6. M. Gruntman, Rev. Sci. Instrum., 68, 3617-3656, 1997.
7. E.C. Roelof, this volume.
8. H.O. Funsten et al., this volume.
9. G.A. Doschek, , W.E. Behring, and U. Feldman, Astrophys. J., 190, L141-L142, 1974.
10. R.R. Meier, Geophys. Res. Lett., 17, 1613-1616, 1990.
11. E. Moebius et al., Nature, 318, 426-429, 1985.
12. G. Gloeckler et al., Science, 261, 70-73, 1993.
13. M.A. Gruntman, J. Geophys. Res., 99, 19213-19227, 1994.
14. L.A. Fisk et al., Geophys. Res. Lett., 24, 93-96, 1997
15. E. Möbius et al., J. Geophys. Res., 103, 257-265, 1998.
16. F. Paresce et al., J. Geophys. Res., 86, 10038-10048, 1983.
17. M.A. Gruntman, Geophys. Res. Lett., 19, 1323-1326, 1992.
18. M. Gruntman, J. Geophys. Res., 106, N.A5, in press, 2001.
19. K.-P. Cheng and F.C. Bruhweiler, Astrophys. J., 364, 573-581, 1990.
20. J. Vallerga, Astrophys. J., 497, 921-927, 1998.
21. M. Landini and B.C. Monsignori Fossi, Astron. Astrophys. Suppl. Ser., 82, 229-260, 1990.
22. S. Bowyer, J. Edelstein, and M. Lampton, Astrophys. J., 485, 523-532, 1997.
23. R.R. Meier, R.R., Space Sci. Rev., 58, 1-185, 1991.